Toxicology Reports 7 (2020) 795–804

Contents lists available at ScienceDirect

Toxicology Reports

journal homepage: www.elsevier.com/locate/toxrep

Involvement of hepatic lipid droplets and their associated proteins in the detoxification of aflatoxin B_1 in aflatoxin-resistance BALB/C mouse

Nour Hammoudeh[a], Chadi Soukkarieh[a], Denis J. Murphy[b], Abdulsamie Hanano[c,*]

[a] Department of Animal Biology, Damascus University, Damascus, Syria
[b] Genomics and Computational Biology Group, University of South Wales, Wales, United Kingdom
[c] Department of Molecular Biology and Biotechnology, Atomic Energy Commission of Syria (AECS), P.O. Box 6091, Damascus, Syria

ARTICLE INFO

Keywords:
Hepatic lipid droplets
BALB/C mice
Detoxification
Aflatoxin B_1

ABSTRACT

The highly potent carcinogen, Aflatoxin B_1, induces liver cancer in many animals including humans but some mice strains are highly resistant. This murine resistance is due to a rapid detoxification of AFB_1. Hepatic lipid droplets (LDs) ultimately impact the liver functions but their potential role in AFB_1 detoxification has not been addressed. This study describes the structural and functional impacts on hepatic LDs in BALB/C mice after exposure to 44 (low dose) or 663 (high dose) μg AFB_1/kg of body weight. After 7 days, the liver of AFB_1-dosed mice did not accumulate any detectable AFB_1 or its metabolites and this was associated with a net increase in gene transcripts of the *AhR*-mediating pathway. Of particular interest, the livers of high-dose mice accumulated many more LDs than those of low-dose mice. This was accompanied with a net increase in transcript levels of LD-associated protein-encoding genes including *Plin2*, *Plin3* and *Cideb* and an alteration in the LDs lipid profiles that could be likely due to the induction of *lipoxygenase* and *cyclooxygenase* genes. Interestingly, our data suggest that hepatic LDs catalyze the *in vitro* activation of AFB_1 into AFB_1-*exo*-8,9-epoxide and subsequent hydrolysis of this epoxide into its corresponding dihydrodiol. Finally, transcript levels of *CYP1A2*, *CYP1B1*, *GSTA3* and *EH1* genes were elevated in livers of high-dose mice. These data suggest new roles for hepatic LDs in the trapping and detoxifying of aflatoxins.

1. Introduction

Aflatoxins (AF) are a group of lipid-derived toxins secreted by certain common fungi including *Aspergillus flavus* and *A. parasiticus* [1–3]. AFs cause both chronic and acute toxicity in humans and animals following consumption of fresh and/or stored AF-contaminated food and feed. In terms of chronic exposure, aflatoxin B_1 (AFB_1), [(6aR,9aS)-2,3,6a,9a-Tetrahydro-4-methoxy-1H,11H-cyclopenta[c]furo[3',2':4,5]furo[2,3-h][1]benzopyran-1,11-dione], is the most toxic form of AFs and is regarded as the most potent environmental carcinogen identified to date, where the exposure to AF is considered as a major causal factor of hepatocellular carcinoma (HCC) [1,3,4]. Acute exposure to AFB_1 also provokes many immunotoxicological effects and alterations in cytokine expression in various animal species [5–7]. Of particular interest, it was shown that AFB_1 affects the expression of lipid metabolizing genes in rat liver, suggesting a potential connection between the AFB_1-induced lipid metabolism and in the long term a possible elevated risk of coronary heart disease [8].

It is well known that the livers of AF-exposed animals are the most active accumulating organs of such toxins, and that the liver plays important roles in the sequestration and biotransformation of AF [9,10]. The hepatic detoxifying capability of AFs, which are highly lipophilic molecules, is ensured by the high intracellular lipid content plus a battery of AF-metabolizing enzymes, most notably microsomal cytochrome P450 s. The biological connection between AF and hepatic lipids has been demonstrated in AFB_1-producing fungal cells where biosynthesis, trafficking and exporting of AFB_1 are strictly modulated by fungal LDs and their associated proteins, especially caleosin/peroxygenase AfPXG [11,12]. Addition of exogenous AFB_1 also causes alterations in plasma and liver lipid levels in exposed animals [8,13,14]. Moreover, the integrated analysis of transcriptomic and metabolomic profiles of AFB_1-induced hepatotoxicity in AFB_1-dosed rats revealed that dysfunction of lipid metabolism was a major metabolic effect, suggesting its potential use as a biomarker for detecting AFB_1-induced acute hepatotoxicity [15].

The efficient and rapid detoxification of AFB_1 requires a set of enzymes that actively metabolize such xenobiotics into more hydrophilic metabolites that are more readily excreted in the urine (via the kidney)

* Corresponding author.
E-mail address: ashanano@aec.org.sy (A. Hanano).

https://doi.org/10.1016/j.toxrep.2020.06.005
Received 23 December 2019; Received in revised form 4 June 2020; Accepted 11 June 2020
Available online 22 June 2020

or in the bile (via the liver). This process varies between different animal species and even between strains of the same species. In the case of common laboratory animals, mice are less sensitive than similar mammalian species such as rats, guinea pigs, and rabbits [16]. Moreover, different inbred mouse strains have differential cellular susceptibilities towards AFB_1, with the BALB/C strain being highly resistant compared with strains such as C57B1/6, B10A and CBA/J [17]. In this context, murine resistance to AFB_1 is related to, but not limited to, the activation of AFB_1 by hepatic α-glutathione-S-transferases (GSTAs), mainly GSTA1 and GSTA3, that rapidly conjugate the AFB_1-*exo*-8,9-epoxide (AFBO) with glutathione forming the AFB_1-exo-glutathione [18], suggesting GSTA as a primary pathway responsible for the detoxification of the AFB_1 in mice [19,20]. Although the AFBO conjugation reaction by GSTA is well characterized in mice, the upstream catalytic activating of AFB_1 is still uncertain. This is because mice do not harbor an ortholog of human CYP3A4 that catalyzes the epoxidation of AFB_1, but do express an ortholog of CYP1A2 that putatively epoxidizes AFB_1 in other mammals, an activity that has never been reported in mice [21], suggesting that the AFB_1-resistance is probably due to the involvement of other pathways.

Mammalian liver cells are well known as active sites of lipid metabolism and this is often reflected in the accumulation, or even hyper-accumulation, of hepatic LDs that typically contain a mainly triacylglycerol core that is surrounded by a specific population of lipid-associated proteins [22–24]. In some cases, hepatic LDs can also serve as storage organelles for lipophilic molecules such as retinoids [25]. Recent studies have demonstrated that the murine hepatic LD proteome is highly dynamic and can undergo rapid compositional changes in response to fasting and refeeding [26]. Hepatic LDs are also implicated in a variety of pathologies, most notably alcohol-related and non-alcolohic fatty liver disease [27,28] and hepatitis C infection [29,30]. However, although LDs have been shown to sequester lipophilic toxins, such as AFB_1, in fungi an analogous role for hepatic LDs has yet to be elucidated in animals.

In this study, we report the involvement of hepatic LDs in the sequestration/trafficking, and possibly, the biotransformation of AFB_1 in BALB/C mice, an AFB_1-resistent strain. To investigate this, hepatic LDs from female mice, exposed to low or high doses of AFB_1 for 7 days, were isolated, purified and characterized with respect to their abundance, size, lipid and protein content. Furthermore, the *in vitro* biotransformation activity of hepatic LDs towards AFB_1 was measured together with transcript abundances of key genes involved in the binding and activation of AFB_1.

2. Materials and methods

2.1. Chemicals, animals, conditions and treatments

Aflatoxin B1 (AFB1) standards from *Aspergillus flavus*, aniline, cumene hydroperoxide and all organic solvents were purchased from Sigma-Aldrich, USA. Oligonucleotides (Table S1) were supplied by the Unit of primers synthesizer at AEC. Twelve-week old female mice, with average weight of 20 g, of BALB/C were obtained from the Breeding Unit for Inbred Mice at the Department of Molecular Biology and Biotechnology, Atomic Energy Commission of Syria (AECS). Mice were housed in clean cages, received feed and clean tap water *ad libitum* and kept under standard 12-h light/dark cycles at 25 ± 2 °C and 40–60 % humidity. Fifteen mice were used in the experiments which were randomly divided into three groups of five animals. Dose-related toxicological effects have been reported in AFB1-exposed laboratory animals notably in mice [17,31–33]. Apparently, these different effects are produced by different pathways. For this reason, in the current work we studied the effects of a low dose (L-dose) and a high dose (H-dos) of AFB1 on the hepatic LDs to determine the responsive and functional capacities of these organelles as a function of AFB1 dose. To do this, groups I and II mice orally received a single 50 µL-dose of corn oil containing 44 (low dose) or 663 (high dose) µg AFB_1/kg of body weight while group III was received a similar dose of corn oil alone [31]. Seven days later, mice were weighed and euthanized. The livers were rapidly removed, rinsed with 0.9 % NaCl, weighed, immediately frozen in liquid nitrogen and stored at -20 °C until further use. All animal experiments were carried out in accordance with the U.K. Animals (Scientific Procedures) Act, 1986 and associated guidelines, EU Directive 2010/63/EU for animal experiments. This study was approved by the AECS Committee of Animal Ethics.

2.2. Extraction and thin layer chromatography (TLC) analysis of aflatoxins

Liver tissue (about one gram) of each experimental mouse was used for analysis of aflatoxin B_1 and its potential biotransformation products. Extraction of AFs was done according to Hanano et al., [12] using 2 mL of chloroform for one hour on a rotary-shaker. Recovery of the extracted AFB_1 was evaluated using a spiked sample with 50 ng AFB_1 for one gram of liver tissue. Thus, the recovered concentration of AFB_1 was considered in the subsequent calculations. The extracts were analyzed by thin layer chromatography (TLC) according to [11]. Samples were spotted onto a C_{18} reverse-phase TLC plate (aluminum sheets 20 × 20 cm, 200 µm layer, Merck, Germany) and the chromatogram developed using a solvent system of chloroform/acetone (90:10, v/v). The detection of AFB1 was compared with a AFB_1-standard point containing 5 ng by spotting 1 µL of AFB_1 standard (5 µg/mL). After development, the spot having a *Rf* value similar to AFB_1 standard (20 µg/mL) was scraped then re-extracted with chloroform and evaporated to dryness under nitrogen. The extract was resuspended with 100 µl chloroform and the concentration of AFB_1 was measured by spectrophotometer at 360 nm.

2.3. Isolation of LDs and microsomal fractions from animal livers

The isolation of LDs was based on their buoyant density, which is less than 1 g/cm^3, by differential centrifugation and using a gradient floating buffer in cooling conditions [34]. The pooled livers of each animal group (about 3 g) were vigorously ground in a mortar and pestle and in the presence of liquid nitrogen. The liver powder was immediately homogenized with 6 mL of homogenization buffer (HB) (50 mM Tris−HCl, 1 mM EDTA, 1 M sorbitol, pH 7.5). The total homogenate was divided into four fractions of 1.5 mL each, transferred into 2-mL microcentrifuge tube and centrifuged at 5000 ×*g* for 15 min at 4 °C. The supernatant (about 1 mL) containing LDs was taken into a clean 2-ml tube, overlaid with an equal volume of floating buffer (FB) (50 mM Tris−HCl, 1 mM EDTA, 1 M sorbitol, pH 7.5) and centrifuged at 21,130 ×*g* for 1 h at 4° C. After centrifugation, three fractions were obtained, an upper creamy floating layer corresponding to the LDs, an infranatant phase corresponding to cytosolic proteins fraction, and a pellet corresponding the microsomal fraction (M). LD fractions were separately and carefully taken and subjected to a one-step washing with 1 mL of FB, then centrifuged at 21,130 ×*g* for 1 h at 4 °C. Finally, the respective fractions, LDs or M, were re-suspended in 100 µL of suspension buffer (50 mM Tris−HCl pH-7.5, 1 mM EDTA pH-8.0 and 10 % glycerol) and stored at 4 °C.

2.4. Characterization of LDs

Isolated LDs were examined under light microscope (Olympus with a mercury light source) at a magnification of ×40. LDs were stained by Nile Blue dye and examined by a fluorescent microscope. For that, the lipophilic Nile Blue dye was dissolved in dimethyl sulfoxide (DMSO) at concentration of 1 mg mL^{-1} then diluted 10× and freshly used to stain 1 µL of LDs for 15 min at room temperature. Stained LDs were immediately examined under a fluorescent microscope (Nikon Ti-U microscope supplied with an Olympus FE-4000 camera) using red and green fluorescence filters (excitation, 545 and 480 nm; emission, 620

and 535 nm, respectively) at ×40 magnification. The concentration of proteins associated with LDs was determined by the Bradford method using bovine serum albumin (BSA) as a standard [35]. The absorbance at 595 nm was measured using a Jenway 6840 spectrophotometer.

2.5. Lipid profile using TLC

The organic mixture (chloroform/acetone) described above for protein precipitation was also used for extraction of lipids from LDs. After centrifugation, the organic phases containing the lipid fraction were transferred into new tubes and evaporated to dryness under nitrogen. Extracted lipids were re-dissolved in 50 µL of the same solvent mixture and analyzed by TLC. Samples were spotted onto a C_{18} reverse-phase TLC plate (aluminum sheets 20 × 20 cm, 200 µm layer, Merck, Germany) and the chromatogram developed using a solvent system of hexane/diethyl ether/acetic acid (80:20:1, v/v/v). Developed TLC plates were dried at room temperature and lipids visualized by iodine vapor.

2.6. Hydroxylation enzymatic activity

The potential fatty acid-oxygenation activities of LD-associated proteins were assayed by a rapid test based on measurement of aniline hydroxylation [11,36]. This was performed by incubating an increasing amount of LDs containing about 0.2, 0.4, 0.8, 1.6, 3.2, 6.4, 12.8 and 25.6 µg of total proteins with 1 mM of aniline in a final volume of 1 mL of 10 mM sodium acetate buffer, pH 5.5 and 20 % (v/v) glycerol. The enzymatic activity was initiated, at room temperature, by adding 4 mM of cumene hydroperoxide as an oxygen donor. The accumulation of hydroxyaniline was spectrophotometrically measured at 310 nm.

2.7. Genes, primers and transcripts analysis

Three sets of genes were selected to study hepatic transcriptional changes in response to the AFB_1. Set I refers to key genes involved in the reception and detoxification pathway of AF, e.g. aryl hydrocarbon receptor (*AhR*), aryl hydrocarbon receptor nuclear translocator (*ARNT*), nuclear factor kappa (*NFκB*), cytochrome P450 1A1(*CYP1A1*), cytochrome P450 1A2 (*CYP1A2*), cytochrome P450 1B1 (*CYP1B1*), glutathione S-transferase α-1 (GSTA1), glutathione S-transferase α-3 (GSTA3) and epoxide hydrolase 1 (EH1). Set II comprises the lipoxygenases (LOX5, LOX12 and LOX15) and cyclooxygenases (COX1 and COX2) catalyzing oxygenation of polyunsaturated fatty acids. Set III contains a collection of genes encoding LD-associated proteins, e.g. Perilipin 2 (*Plin2*), Perilipin 3 (*Plin3*), Perilipin 4 (*Plin4*), Perilipin 5 (*Plin5*), Cell death-inducing DFFA-like effector b (*Cideb*), Cell death-inducing DFFA-like effector c (*Cidec*), peroxisome proliferator-activated receptor α (*Ppara*), peroxisome proliferator-activated receptor gamma (*Pparg*) and peroxisome proliferator-activated receptor delta (*Ppard*). Gene expression was normalized to that of a set of reference genes, i.e. actin-beta (*Actb*), ribosomal protein L13a (*RPL13a*), hypoxanthine phosphoribosyl transferase 1 (*Hprt1*) and succinate dehydrogenase complex flavoprotein subunit A (*SdhA*). Table 1 summarizes gene name, NCBI-accession number, forward and reverse oligonucleotides and expected amplicon size.

Changes in relative transcriptional abundance of three sets of genes in response to AFB1 exposure were analysed by reverse-transcription quantitative PCR (RT-qPCR) as described [37]. For RNA extraction, 30 mg of liver from each animal group were finely ground in the presence of liquid nitrogen and the total RNA was extracted using an RNeasy kit according to the manufacturer's instructions (Qiagen, Germany). DNA traces were removed by treating the samples for 1 h at 37 °C with 2 U of RNase-free RQI DNase (Promega, USA). RNAs were diluted to 50 ng/µL using RNase-free water and stored at - 80 °C. Aliquots of 1 µg total RNA were used for first-strand cDNA synthesis using M-MLV RT (Invitrogen), for more details please refer to Hanano et al., [38]. Real-time PCR was performed in 48-well plates using an AriaMx Real-time PCR System from Agillent technologies, USA. In brief, 25 µL reaction mixtures contained 0.5 µM of each specific oligonucleotide primer for the target and reference genes, 12.5 µL of SYBR Green PCR mix (Bio-Rad, USA) and 100 ng cDNA. qPCR conditions were as described before [36]. Each point was replicated in triplicate and the average of C_T was taken for calculation of the relative quantification $RQ = 2^{(-\Delta\Delta CT)}$.

2.8. In vitro biotransformation of AFB_1

The activity of LD and microsome fractions isolated from control and AFB_1-treated mice were assayed for biotransformation of AFB_1. An aliquot of 100 µL containing about 15 µg protein from each fraction was separately incubated with 15 ng of standard AFB_1 pre-dissolved in DMSO at 37° C for 1 h with gentle shaking (~200 rpm). After incubation, the AFB1 and its metabolites were immediately extracted with 1 mL of chloroform by vigorous vortexing for 15 min and a brief centrifugation at 14,500 rpm for 5 min. The organic phase was evaporated under nitrogen and resolved in 50 µL chloroform for further analysis. AFB_1 metabolites were analyzed by TLC onto a C_{18} reversed-phase plate (Aluminum sheets 20 × 20 cm, 200 µm layer, Merck, Germany) using a solvent system of chloroform/acetone (9:1 v/v). Plates were examined under UV light at 365 nm. UV-florescent metabolites of AFB_1 was scraped and re-extracted from the silica gel by 0.5 mL of chloroform as described above.

2.9. Detection of AFB_1 metabolites by HPLC-FD

Purified AFB_1 and its metabolites were analyzed on a Waters Alliance e2695 HPLC system (Waters Corporation, Milford, MA, USA) equipped with a 2475 fluorescence detector. Samples were run at 25 °C on a ZORBAX SB-C_{18} column. The mobile phase, the gradient schedule, and detection conditions were as described previously [39]. The flow rate was 1 mL/min and the injection volume was 50 µL. Fractions corresponding to each metabolites were collected and the spectral characterization of both metabolites, AFB_1 8,9-epoxide and AFB_1-*exo*-8,9-dihydrodiol, was performed by UV- and Fluorescent-spectroscopy as described by Johnson et al., [40]. First, absorbance ($Abs_{300-400}$) spectra were recorded using a Jenway 6840 spectrophotometer with a wavelength range from 300 to 400 nm. Fluorescence spectra were recorded using a Varian SF-330 spectrofluorometer, with a wavelength range from 350 to 550 nm.

2.10. Statistics

All data presented were expressed as means ± standard deviation (SD). Statistical analysis was performed using IBM SPSS statistics 23p4. Statistical significance between control and treatments was evaluated by ANOVA.

3. Results

3.1. Detection of AFB_1 and its metabolites in mouse liver

AFB_1 and its metabolites were extracted from livers of healthy and AFB_1-dosed animals and analyzed by TLC. No blue-fluorescent spots were detected in the extracts of livers from L- (low AF doses) and H-dosed (high AF doses) animals corresponding to the AFB_1 standard *Rf* of 0.316 (Fig. 1 A). The rapid detoxification of AFB_1 was accompanied with an increase in transcripts levels of selected genes involved in cytotoxicological responses of animal cells towards aflatoxins, i.e., aryl hydrocarbon receptor (*AhR*), aryl hydrocarbon receptor nuclear translocator (*ARNT*), nuclear factor kappa (*NFκB*). These gene products potentially regulate expression of genes involved in the initial steps of AFB_1-activation. The relative quantification of genes transcripts, shown

Table 1
Names and nucleotide sequences of primers used in this study.

Name	Accession #	Forward Primer	Reverse Primer	Amplicon
Actb	NM_007393.5	TCCAGGCTGTGCTGTCCCTGT	ACGCAGGATGGCGTGAGGGA	125
RpL13a	NM_009438.5	CGAGCCCCCAGCCGCATTTT	AGCAGGGACCACCATCCGCT	147
Hprt1	NM_013556.2	GCAGCGTTTCTGAGCCATTG	TCATCGCTAATCACGACGCT	172
SdhA	NM_023281.1	ACCTGACAGCTACAGGACCA	GACAAAGTCTGGCGCAACTC	173
AhR	NM_001314027.1	TCCACCGCTGCTGGTGAGGT	CTGCTGCTGGCAAGCCGAGT	117
ARNT	NM_001037737.2	GCTCATTCCCTCCTAACCCC	GTCTTGGCTGTAGCCTGGG	217
NFkB	NM_001177369.1	CGCCACCTGCTGATGGCACA	GCAGAGGCGTCTGGTGCAGG	163
CYP1A1	NM_009992.4	CCTGTGGTGGTGCTGAGCGG	CAGGGCATTCTGGGCCAGGC	183
CYP1A2	NM_009993.3	TCACTAACGGCAAGAGCATGA	TGGCTGACTGGTTCGAAGTG	223
CYP1B1	NM_009994.1	GCGACGATTCCTCCGGGCTG	CTCATGCAGGGCAGGCGGTC	193
GSTA1	NM_008181	CCCCCAGACCAAAGAGAAGCCA	ACCCTGGTCAGCCTGTTGCC	131
GSTA3	NM_001077353	TACCCCCACATGCCCCCTGA	AGCCCTGCTCAGCCTGTTGC	144
EH1	NM_001312918	ATTCCCTGACCCCTCTCCTGGG	CCCACAGTGTCCGGCTTGGT	160
LOX5	NM_009662.2	CCCCTGGAGAGAGTAACCCA	TGAAAAGGGGATGCACAGCA	192
LOX12	NM_007440.5	TTTGACTTCGACGTTCCCGA	GGAGGCTCAGGATTCCCTCT	181
LOX15	XM_006532036.3	GAAGATGTAACCCACCACGTTC	CCAAGACAGAGGAACACAGGG	174
COX2	NM_011198.4	AACCGCATTGCCTCTGAAT	CATGTTCCAGGAGGATGGAG	130
COX1	XM_017316496.1	TTTCTCTCAGCCTCTTCGGG	GGTTCAATCCCTCCCAGCTC	244
Plin2	NM_007408.3	ACCGTGACCTCTGCGGCCAT	TCGCCCCAGTTACGGCACCT	181
Plin3	NM_025836.3	CAGCAGCAGCGACAGGAGCA	AGCCTCTGGTCCACACCCTGT	191
Plin4	NM_020568.3	AAGGCACAGCGCAGATGGGT	ACAGCCCCTGTGAGCCCTGT	187
Plin5	NM_025874.3	GCGCAGCGTGGATGCTCTACA	GGCCCGCAGGACCAAATCCA	145
Cideb	NM_009894.3	AGCCTTCAACCCCAATGGCCTG	ACACGGAAGGGTCGCTGAGGT	105
Cidec	NM_178373.4	TGCTCCGCTGGACCCTCTTCA	GCTTGGCCTTGGCAGGCTGT	117
Ppara	NM_011144.6	TCGGCTGAAGCTGGTGTACGA	CCCGACAGACAGGCACTTGTG	106
Pparg	NM_001127330.2	CAGGTTTGGGCGGATGCCACA	TCGCCCTCGCCTTGGCTTTG	167
Ppard	NM_011145.3	AAAGACGGGCTGCTGGTGGC	CGCGATGAAGAGCGCCAGGT	162

in Fig. 1 B, reveals a brief raise in *AhR* gene transcript levels while those of *ARNT* and *NFkB* increased by 27.9 and 5.5-fold respectively. These results show that, after seven days, the livers of AFB_1-dosed mice do not accumulate detectable traces of AFB_1 or its metabolites, possibly due to a rapid and efficient hepatic AFB_1-detoxifying system mediated by the AhR pathway.

3.2. The exposure to AFB1 modulates the number and composition of hepatic LDs in a dose-dependent manner

LDs were firstly fractioned from liver of healthy mice. The quality and purity of LD fractions were examined by light and fluorescence microscopy. As shown in Fig. 2, isolated LDs appeared as intact spherical structures under the light microscopy and confirmed by Nile Blue staining under fluorescence microscopes, where the stained LDs were highly fluorescent in green and in red under according to the filter used. The LDs were subsequently fractioned from livers of control (Fig. 3 A I and II) and AFB1-exposed animals of L-dose (Fig. 3 B I and II) and H-dose (Fig. 3 C I and II), respectively. The LD count was about of 60×10^4 per mL in the fraction isolated from the liver of control mice (Fig. 3 A III), decreased to about of 45×10^4 per mL L-dose mice (Fig. 3 B III), but considerably increased to about of 148×10^4 per mL in H-dose mice (Fig. 3 C III). The concentration of LD-associated proteins was much lower in L-dose fractions, not exceeding 0.22 mg mL (Fig. 3 A IV), but was considerably higher in the H-dose fraction, reaching about 2.5 mg mL^{-1} (Fig. 3 B IV). This compared to an LD-associated protein concentration in the control fraction of about 1.8 mg/mL (Fig. 3 C IV).

Unexpectedly, although the concentration of LD-associated proteins decreased in L-dose fraction, we did not detect any significant change in the transcript levels of their respective genes (Fig. 3 D). In contrast, the increase in the concentration of LD-associated proteins in the H-dose fraction was accompanied by increases in the transcript levels of key LD-associated proteins encoding genes, notably *Plin2*, *Plin3* and *Cideb*. The transcript levels of these genes increased about of 25-, 9- and 6-fold, respectively (Fig. 3 D). These data indicate that exposure of mice to AFB1 affects the accumulation of hepatic LDs and possibly their proteomic signature in a dose-dependent manner. Also, while, a chronic dose of AFB_1 leads to a net decrease the hepatic LDs, an acute dose stimulates their accumulation.

3.3. Exposure to AFB1 affects the lipid profile of hepatic LDs

Both the composition of LD-associated proteins and the nature of their lipidic core can play important roles in the diverse biological functions of LD organelles. The lipid composition was evaluated for each fraction of LDs using TLC. Compared to controls, the lipidic profile of LDs extracted from L-dose set contained only small amounts of TAG and a surprising amount of MAG (Fig. 4 A). However, the LD lipids of H-dose mice contained the expected main five classes, namely as MAG, DAG, TAG, free fatty acids (FFA) and sterol esters (SE) albeit with reduced relative amounts of MAG and DAG. Polyunsaturated fatty acids and their oxygenated metabolites, collectively termed oxylipins, that are present in the lipidic core of LDs are crucial for their biological functions. Therefore, the expression of selected genes involved in the oxygenation of polyunsaturated fatty acids pathways was examined, i.e., Lipoxygenases (*LOX5*, *LOX12* and *LOX15*) and Cyclooxygenases (*COX1* and *COX2*) respectively catalyzing the formation of leukotrienes, prostaglandins and thromboxanes. As shown in Fig. 4 B transcripts levels of these genes varied as a function of AFB_1 dose. In particular, transcripts levels of *LOX5*, *LOX12*, *LOX15* and *COX2* were significantly more induced in the livers of L-dose animals while *COX1* transcripts were only increased in the livers of H-dose animals. Furthermore, the induction of *LOX* genes in the livers of L-dose animals was synchronized with a similar induction of the hyroperoxide reductase activity of the LDs fraction prepared from the livers of L-dose animals. Compared to controls, this activity was about of 0.2 Abs_{310} greater in the LDs of L-dose animals and about of 0.1 Abs_{310} less in the LDs of H-does animals (Fig. 4 C). These results indicate that exposure of mice to AFB_1 modifies, in a dose-dependent manner, the lipid profile of hepatic LDs and the expression of key oxylipin biosynthesis pathway genes.

3.4. Purified hepatic LDs can catalyse the biotransformation of AFB_1 in vitro

The sequestration of AFB_1 into LDs of fungal cell was recently demonstrated [11]. However, the biochemical connection between the

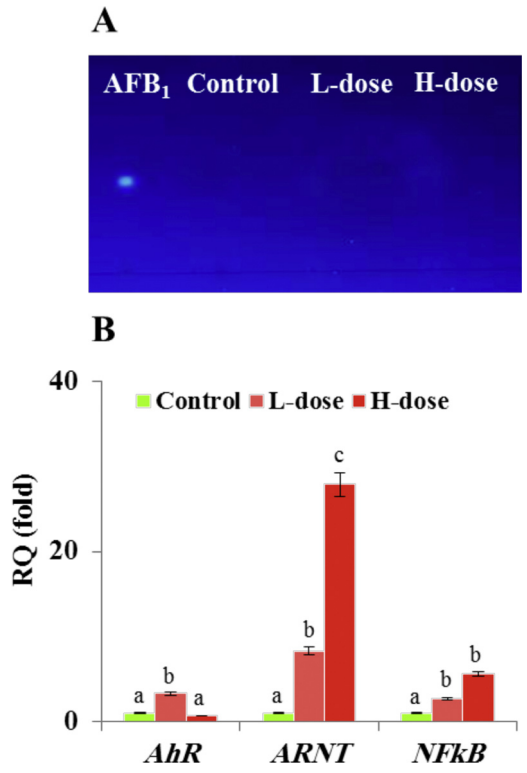

Fig. 1. Hepatic metabolism of AFB_1 and activation of genes expressed from the AhR-mediating pathway. **A**, TLC-analysis of AFB_1 extracted from livers of control and AFB_1-treated mice at low (L) or high doses (H). The *Rf* values of samples were compared to the *Rf* of an AFB_1 standard. **B**, Relative quantification (RQ) data of AhR, ARNT and NFkB gene transcripts as described in Methods. Two independent measurements were taken of cDNAs prepared from three individual animals for each treatment. For each dose, the expression level for a given gene in the control was defined as 1 and the corresponding abundance changes in L- and H-dosed animals were calculated. Uppercase letters indicate significant differences in the genes expression between control and AFB_1-dosed animals, where columns with different upper case letters (a,b) were statistically significant ($^{b}P < 0.05$) and (a,c) were statistically very significant ($^{c}P < 0.01$), as determined by the ANOVA test.

AFB_1 and LDs in animal cells has yet to be elucidated. To determine whether a such connection exists, AFB_1 was incubated with LD fractions from livers of control, L-dose and H-dose mice. The TLC data in Fig. 5 show that LD fractions from L-dose and H-dose mice metabolized AFB_1 similarly to each other but differently from controls. Most of the AFB_1 was still intact after incubation with control LDs but it was metabolized in the treated mice into two derivatives (1 and 2) with *Rf* values of 0.57 and 0.44, respectively (Fig. 5 A). To characterize the AFB_1 metabolites, the two spots were re-extracted and separately analyzed by TLC (Fig. 5 B). In parallel, the purified metabolites were subsequently analyzed by HPLC-FD, where the less retained metabolite was eluted at retention time (Rt) of 8.75, while the other metabolite was eluted at Rt of 20.58, compared with the intact AFB1 that has a Rt of 25.62 (Fig. 5 C). In respect to their Rt values, compared with those that have been earlier reported, the both metabolites could probably correspond to AFB_1-*exo*-8,9-dihydrodiol and AFB_1-*exo*-8,9-epoxide, respectively. To gain more information about the biochemical identity for these metabolites, both was characterized in the respect to their respective spectral features and this was summarized in Table 2. First, in term of absorbance changes ($Abs_{300-400}$), the absorbance spectra indicate a λ_{max} of 348 nm for the AFB_1-*exo*-8,9-epoxide and a λ_{max} of 364 nm for the hydrolysis product, AFB_1-*exo*-8,9-dihydrodiol. A comparison of spectra shows that the widest change in *Abs* upon hydrolysis of the epoxide was between 370 and 390 nm. Moreover, the difference in the fluorescence spectra between the AFB_1-*exo*-8,9-epoxide and the AFB_1-*exo*-8,9-dihydrodiol was significant. The λ_{max} for AFB_1-*exo*-8,9-epoxide was 382 nm, however, the λ_{max} for AFB_1-*exo*-8,9-dihydrodiol was 454 nm. In addition, compared to their levels in controls, transcripts levels of *CYP1A2*, *CYP1B1*, *GSTA3* and *EH1* were much higher in the H-dose animals (2.1, 5.02, 3.75 and 4.94-fold, respectively) (Fig. 5 D). These data suggest that hepatic LDs of AFB_1-dosed can effectively catalyze the biotransformation of AFB1 and this activity conducts the transformation of AFB_1-*exo*-8,9-epoxide into its corresponding dihydrodiol.

4. Discussion

Aflatoxin B_1 (AFB_1) is a highly potent poison that contaminates both human foods and animal feedstuffs and particularly targets the liver of exposed individuals. The acute-hepatotoxicity of AFB_1 is typified by the induction of apoptosis and genotoxicity in humans, with a potential additional risk of hepatocellular carcinoma [41–44]. Minimizing the cytotoxicity of AFB_1 is dependent on the presence of an efficient hepatic detoxifying system that ensures a rapid elimination of AFB_1. In this report, we describe new evidence for the involvement of hepatic LDs in the detoxification of an acute dose of AFB_1 in the AF-resistant strain of BALB/C mouse. The results show that, after seven days, the livers of AFB_1-dosed mice did not accumulate detectable traces of AFB_1 or its potential metabolites and that this could be due to a rapid and efficient hepatic AFB_1-detoxifying system mediated by the AhR pathway. These data support earlier reports of the rapid elimination of AFB_1 from liver tissue of BALB/C mouse and its correlation with a specific transcriptional pattern of the AhR-mediating pathway [17,45]. Such a rapid elimination of AFB_1 is in accordance with a recent report of increased transcripts levels of aryl hydrocarbon receptor (*AhR*), aryl hydrocarbon receptor nuclear translocator (*ARNT*) and nuclear factor kappa (*NFκB*), which are key genes implicated in the initial steps of AFB_1-activation [46].

Our data also indicate that the exposure of mice to AFB_1 affects the accumulation of hepatic LDs and possibly their proteomic signature in a dose-dependent manner. While, a chronic dose of AFB_1 caused a net decrease in hepatic LD numbers, an acute dose stimulated their accumulation, suggesting involvement of two different pathways relating to AFB_1 detoxification by hepatic LDs. Interestingly, dose-differential responses to AFB_1 have been demonstrated by several groups [19,32]. Although acute aflatoxicosis is less common than the chronic condition, it can occur occasionally as shown in episodes correlated with acute-dose-specific gluconeogenesis and lipid metabolism disorders [15]. The

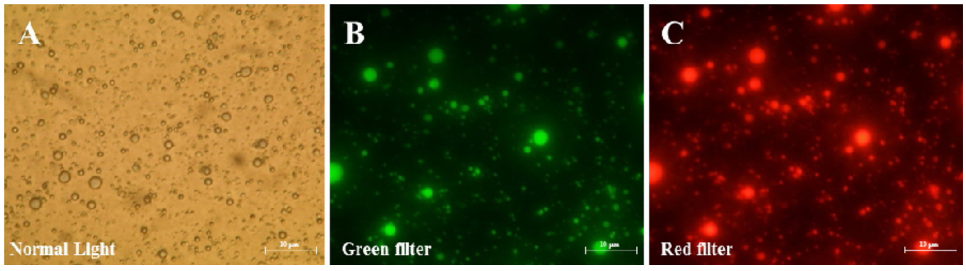

Fig. 2. Detection of hepatic LDs fraction under light and fluorescent microscopy. **A**, micrograph of LDs fraction from liver of control animal under normal light at ×40 magnification. **B** and **C**, micrographs of LDs after staining by Nile Blue. Stained LDs were examined under a fluorescent microscope (Nikon Ti-U microscope supplied with an Olympus FE-4000 camera) using green and red fluorescence filters (excitation, 515-560 nm; emission, > 590 nm) at magnification of ×100. Bars represent 10 μm.

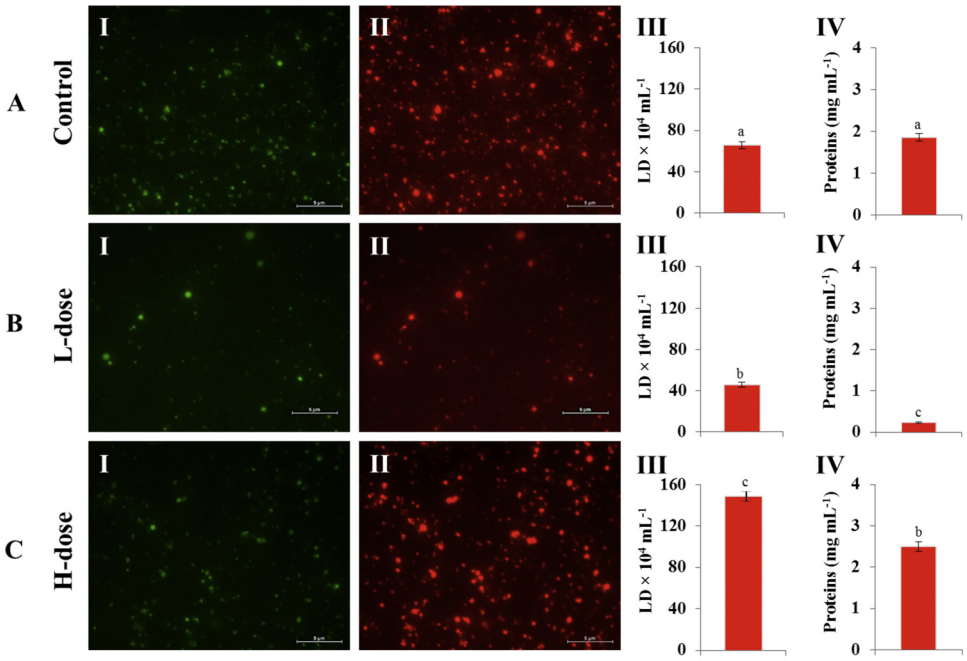

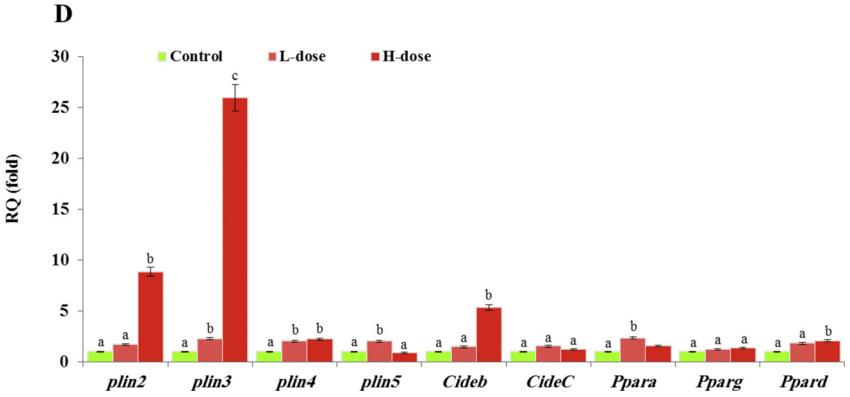

Fig. 3. AFB_1 affects accumulation of hepatic LDs and expression of their associated proteins in a dose-dependent manner. **A, B** and **C**, micrographs of LD fractions from control, L and H dosed animals under a fluorescent microscope using green (panel I) and red (panel II) filters at magnification of ×40. Bars represent 5 μm. LD counts and the concentration of their associated proteins are presented for each fraction in panel III and IV, respectively. **D**, trancript levels of LD-associated protein-encoding genes analysed by qRT-PCR. Two independent measurements were taken of cDNAs prepared from three individual animals for each treatment. For each dose, the expression level for a given gene in the control was defined as 1 and corresponding abundance changes in L- and H-dosed animals calculated. Uppercase letters indicate significant differences in the genes expression between control and AFB_1-dosed animals, where columns with different upper case letters (a,b) were statistically significant (($^b P < 0.05$) and (a,c) were statistically very significant ($^c P < 0.01$), as determined by the ANOVA test.

determination of the proteomic signature of LDs requires isolation of highly pure LDs fractions. The purity of LDs in this study was confirmed by two sequential washings to eliminate endoplasmic reticulum-associated proteins contaminants as previously discussed [26]. Several previous investigations have highlighted the dynamic character of LDs and the often rapid changes in LD proteomes in response to a wide range of developmental, environmental, physiological and pathophysiological factors [24,26,47–50]. Perilipins are major components of the mammalian LD proteome and are involved in their formation and subsequent functions [51]. In this context, our data showed that expression of certain perilipins, notably *Plin2* and *Plin3* was induced by TCDD which is in line with earlier reports indicating the essential role of these perilipins in the structural stability of LDs [52]. It is suggested that Plin2 promotes LD formation and thereby protects the

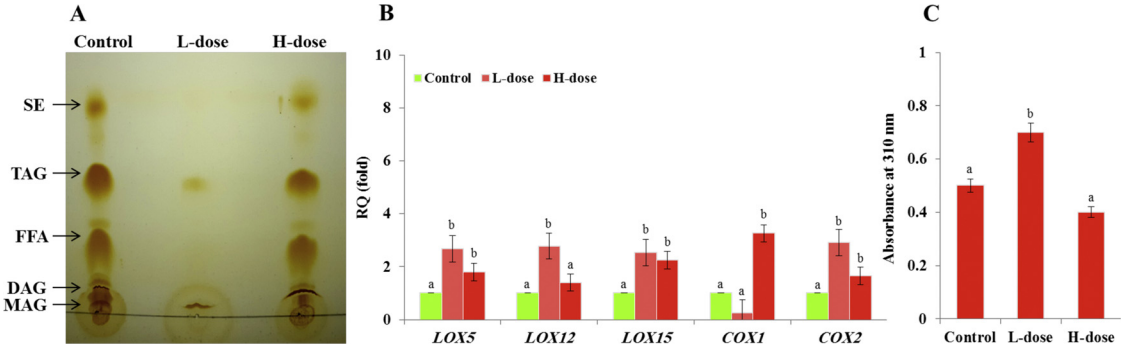

Fig. 4. AFB_1 modifies the lipid profile of hepatic LDs and the expression of key genes in the oxylipin biosynthesis pathway. **A**, TLC-analysis of neutral lipids of hepatic LD isolated from control, low- (L)- and high- (H)-dosed animals. Abbreviations: MAG, monoacylglycerol; DAG, diacylglycerol; FFA, free fatty acids; TAG, triacylglycerol; SE; sterol ester. **B**, relative quantification of transcripts for key genes of the oxylipin biosynthesis pathway. **C**, enzymatic activity of the LD-associated oxygenases measured by differential absorption at 310 nm. For each set, two independent measurements were taken for three individual animals. Uppercase letters indicate significant differences in the genes expression or enzymatic activity between control and AFB_1-dosed animals ($^b P < 0.05$).

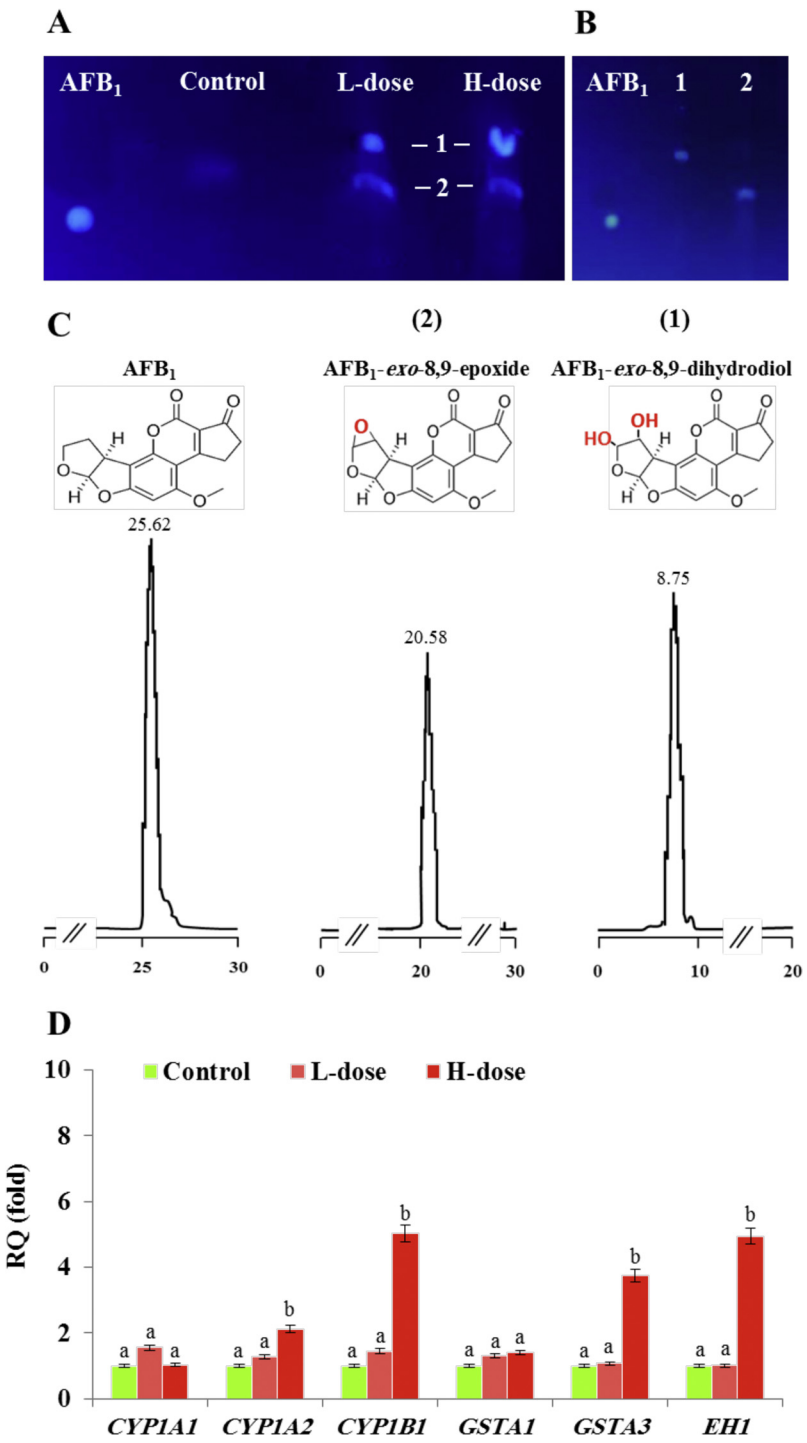

Fig. 5. Trapping and biotransformation of AFB_1 by hepatic LDs. **A**, TLC-separation of AFB_1 metabolites (spots 1 and 2) resulting from *in vitro* incubation of standard AFB_1 with a pure fraction of liver LDs from control, L and H dosed mice. B, sequential TLC-analysis for the purified metabolites 1 and 2 compared to AFB_1 standard. **C**, HPLC-FD-analysis of AFB_1 and its metabolites 1 and 2 compared with their respective standards with retention times of 25.62, 20.58 and 8.75, respectively. **D**, relative quantification of transcripts for key genes involved in the activation and biotransformation of AFB_1. Two independent measurements were taken of cDNAs prepared from three individual mice for each treatment. For each dose, the expression level for a given gene in the control was defined as 1 and the corresponding abundance changes in L- and H-dosed animals were calculated. Uppercase letters indicate significant differences in the genes expression between control and AFB_1-dosed animals ($^b P < 0.05$).

lipidic core from lipolysis [53,54]. More interestingly, the activation of Plin2 is normally modulated by peroxisome proliferator-activated receptor α (PPARα) and γ (PPARγ) signaling in various tissues, including the liver and kidney [55–57] which is in agreement with our data showing a brief but significant increase in PPARα transcripts. Moreover, our data demonstrate that TCDD induced the expression of Cideb, a member of cell death activator proteins. This observation is of special importance regarding the biological roles of this protein in mediating of LD growth as well as LD-LD interactions, especially in adipocytes, and in promoting exchange of lipids and other components between LDs [58].

In addition to their protein profiles, our data indicate that exposure to AFB_1 also modifies LD lipid profiles and expression of key oxylipin biosynthesis pathway genes. In this context, lipids have been used as biomarkers to assess cell status under various conditions and even as clinical diagnostic tools. For example, specific lipids associated with diabetes and obesity are routinely used in diagnosis [59,60]. The accumulation and lipid patterns of adipocyte LDs was found to be conditioned by several factors and this was mediated via fatty acid uptake or lipogenesis [61]. We also found that the acute-AFB_1-dosed mice had high level of hepatic TAGs. This is in line with reports showing that acute exposure to AFB_1 increased levels of plasma and liver lipids notably TAGs [8,14]. Our results show that AFB_1-related changes in LDs lipid profiles were accompanied by increasing transcript levels of some fatty acid metabolizing genes, notably LOXs and COXs, which were differentially induced as a function of AFB_1 dose. In agreement with

Table 2
Values of R_f, Rt and λ_{max} of AFB_1 metabolites.

Metabolite	Absorbance (λ_{max})	Fluorescence (λ_{max})	TLC (R_f)[a]	HPLC-FD (Rt)[b]	Reference
Metabolite 1	364	454	0.57	8.75	This study
AFB1-*exo*-9,8-dihydrodiol	365	450		12.2	1,2
Metabolite 2	348	382	0.44	20.58	This study
AFB1-*exo*-9,8-epoxide	350	380		21.20	1,2,3,4

1 [64].
2 [40].
3 [39].
4 [74].
[a] Retention factor in TLC.
[b] Retention time in HPLC-FD.

this, several lines of evidence have demonstrated induction of LOX and COX genes in response to inflammatory stimuli and to high risk of carcinogenesis [62,63].

Interestingly, our results show that the purified LDs can catalyze the biotransformation of AFB_1 into the corresponding dihydrodiol and this activity is enhanced in the LD fraction isolated from AFB_1-dosed animals. Indeed, the biochemical identities of the resulting metabolites, as suggested as AFB_1-*exo*-8,9-dihydrodiol and AFB_1-*exo*-8,9-epoxide, can be supported by several lines of analytical evidence. First, each metabolite was eluted from HPLC-FD system at retention time that is relatively similar to the values reported before [39,64]. More specifically, the purified metabolites exhibited absorbance and fluorescence spectral features that are identical to those of AFB_1-*exo*-8,9-dihydrodiol and AFB_1-*exo*-8,9-epoxide [40]. The formation of these metabolites under the action of a purified fraction of hepatic LD necessity the presence of the enzymes that are typically involved in a such process, i.e., an AFB_1-epoxidase and possibly a hepatic AFB_1-epoxide hydrolase. The affinity of AFB_1 for LDs has been experimentally proven in several previous studies [11]. However, the integration of AFB_1-metabolizing enzymes into the LDs was unexpected. Indeed, the enrichment of LDs with such enzymes could be explained by two possibilities; the first is that AFB_1-metabolizing enzymes, or a subset of them, are LD-associated proteins, and the second is that these enzymes, or a subset of them, are stored/trapped in the LDs. Whatever the method of association, there are multiple reports of the presence of CYP450 proteins in hepatic LDs and their increasing abundance increased during diet-induced hepatic steatosis [65–67].

Although our observations suggested that the biotransformation of AFB_1 by LDs is likely mediated by an AFB_1-epoxidase and a microsomal AFB_1-epoxide hydrolase, the involvement of hepatic α-glutathione S-transferases, especially GSTA3, in this process is also possible. This can be concluded by the net increase in the level of gene transcripts that we detected in the liver of highly AFB_1-dosed mice. Accordingly, the most likely mechanism for the extreme sensitivity of some animal species and humans is due to the absence of functional hepatic GSTA3 and its analogs [68–70]. As a result, the AFB_1-epoxide remains freely active to form DNA and RNA adducts inducing mutations, block transcription and/or alter translation [71,72]. The functional implication of GSTA3 in the detoxification of AFB_1 was also clearly demonstrated in the GSTA3-knockout mice which, when exposed to AFB_1, exhibited a strong induction of hepatocellular carcinomas or cholangiocarcinomas [73]. Inversely, AFB1-resistent wild-type mice strains harbored a high activity of GSTA3 which is consistent with our observations in this study [19].

5. Conclusions

This study highlights the potential role of hepatic LDs in the rapid detoxification of AFB_1 when BALB/C mice, known for high resistance to AFB1, were exposed to an acute dose of AFB_1 for 7 days. An acute dose of AFB_1 induced accumulation of LDs in the livers of exposed animals. Of particular interest, purified fraction of LD was likely able to detoxify AFB_1 *in vitro* into the corresponding dihyrodiol. Although the current work presents some of interesting indication on a possible involvement of hepatic LDs in the biotransformation of AFB_1, future research is required for better characterization of this new mechanism. So, we suggest to pay a particular attention to the hepatic LDs and their potential roles in the detoxification of AFB_1. It also opens up new horizons for additional roles of LDs in the sequestration, biotransformation and excretion of lipid-soluble toxins in general.

Declaration of Competing Interest

The authors declare no conflict of interest.

Acknowledgements

We would like to thank Prof. Dr. Ibrahim OTHMAN, Director General of the AECS and Dr. Nizar MIRALI, Head of the Department of Molecular Biology and Biotechnology at the AECS for their crucial support.

Appendix A. Supplementary data

Supplementary material related to this article can be found, in the online version, at doi:https://doi.org/10.1016/j.toxrep.2020.06.005.

References

[1] J. Yu, P.K. Chang, K.C. Ehrlich, J.W. Cary, D. Bhatnagar, T.E. Cleveland, G.A. Payne, J.E. Linz, C.P. Woloshuk, J.W. Bennett, Clustered pathway genes in aflatoxin biosynthesis, Appl. Environ. Microbiol. 70 (2004) 1253–1262.
[2] G.S. Shephard, Impact of mycotoxins on human health in developing countries, Food Addit. Contam. Part A Chem. Anal. Control Expo. Risk Assess. 25 (2008) 146–151.
[3] J. Yu, Current understanding on aflatoxin biosynthesis and future perspective in reducing aflatoxin contamination, Toxins (Basel). 4 (2012) 1024–1057.
[4] P. Cai, H. Zheng, J. She, N. Feng, H. Zou, J. Gu, Y. Yuan, X. Liu, Z. Liu, J. Bian, Molecular mechanism of aflatoxin-induced hepatocellular carcinoma derived from a bioinformatics analysis, Toxins (Basel). 12 (2020).
[5] J. Mehrzad, B. Devriendt, K. Baert, E. Cox, Aflatoxin B(1) interferes with the antigen-presenting capacity of porcine dendritic cells, Toxicol. In Vitro 28 (2014) 531–537.
[6] A. Mohammadi, J. Mehrzad, M. Mahmoudi, M. Schneider, Environmentally relevant level of aflatoxin B1 dysregulates human dendritic cells through signaling on key toll-like receptors, Int. J. Toxicol. 33 (2014) 175–186.
[7] B. Grenier, T.J. Applegate, Modulation of intestinal functions following mycotoxin ingestion: meta-analysis of published experiments in animals, Toxins (Basel). 5 (2013) 396–430.
[8] O.A. Rotimi, S.O. Rotimi, C.U. Duru, O.J. Ebebeinwe, A.O. Abiodun, B.O. Oyeniyi, F.A. Faduyile, Acute aflatoxin B1 - induced hepatotoxicity alters gene expression and disrupts lipid and lipoprotein metabolism in rats, Toxicol. Rep. 4 (2017) 408–414.
[9] N.Y. Zhang, M. Qi, X. Gao, L. Zhao, J. Liu, C.Q. Gu, W.J. Song, C.S. Krumm, L.H. Sun, D.S. Qi, Response of the hepatic transcriptome to aflatoxin B1 in ducklings, Toxicon. 111 (2016) 69–76.
[10] L.H. Sun, M.Y. Lei, N.Y. Zhang, X. Gao, C. Li, C.S. Krumm, D.S. Qi, Individual and combined cytotoxic effects of aflatoxin B1, zearalenone, deoxynivalenol and fumonisin B1 on BRL 3A rat liver cells, Toxicon. 95 (2015) 6–12.

[11] A. Hanano, M. Alkara, I. Almousally, M. Shaban, F. Rahman, M. Hassan, D.J. Murphy, The peroxygenase activity of the Aspergillus flavus caleosin, AfPXG, modulates the biosynthesis of aflatoxins and their trafficking and extracellular secretion via lipid droplets, Front. Microbiol. 9 (2018) 158.
[12] A. Hanano, I. Almousally, M. Shaban, E. Blee, A caleosin-like protein with peroxygenase activity mediates Aspergillus flavus development, aflatoxin accumulation, and seed infection, Appl. Environ. Microbiol. 81 (2015) 6129–6144.
[13] A.A. El-Nekeety, S.H. Abdel-Azeim, A.M. Hassan, N.S. Hassan, S.E. Aly, M.A. Abdel-Wahhab, Quercetin inhibits the cytotoxicity and oxidative stress in liver of rats fed aflatoxin-contaminated diet, Toxicol. Rep. 1 (2014) 319–329.
[14] L. Zhang, Y. Ye, Y. An, Y. Tian, Y. Wang, H. Tang, Systems responses of rats to aflatoxin B1 exposure revealed with metabonomic changes in multiple biological matrices, J. Proteome Res. 10 (2011) 614–623.
[15] X. Lu, B. Hu, L. Shao, Y. Tian, T. Jin, Y. Jin, S. Ji, X. Fan, Integrated analysis of transcriptomics and metabonomics profiles in aflatoxin B1-induced hepatotoxicity in rat, Food Chem. Toxicol. 55 (2013) 444–455.
[16] M.S. Monson, R.A. Coulombe, K.M. Reed, Aflatoxicosis: lessons from toxicity and responses to aflatoxin B1 in poultry, Agriculture 5 (2015) 742–777.
[17] R.M. Almeida, B. Correa, J.G. Xavier, M.A. Mallozzi, W. Gambale, C.R. Paula, Acute effect of aflatoxin B1 on different inbred mouse strains II, Mycopathologia 133 (1996) 23–29.
[18] V. Dohnal, Q. Wu, K. Kuca, Metabolism of aflatoxins: key enzymes and interindividual as well as interspecies differences, Arch. Toxicol. 88 (2014) 1635–1644.
[19] Z. Ilic, D. Crawford, D. Vakharia, P.A. Egner, S. Sell, Glutathione-S-transferase A3 knockout mice are sensitive to acute cytotoxic and genotoxic effects of aflatoxin B1, Toxicol. Appl. Pharmacol. 242 (2010) 241–246.
[20] K.H. Kensler, S.L. Slocum, D.V. Chartoumpekis, P.M. Dolan, N.M. Johnson, Z. Ilic, D.R. Crawford, S. Sell, J.D. Groopman, T.W. Kensler, et al., Genetic or pharmacologic activation of Nrf2 signaling fails to protect against aflatoxin genotoxicity in hypersensitive GSTA3 knockout mice, Toxicol. Sci. 139 (2014) 293–300.
[21] E.P. Gallagher, L.C. Wienkers, P.L. Stapleton, K.L. Kunze, D.L. Eaton, Role of human microsomal and human complementary DNA-expressed cytochromes P4501A2 and P4503A4 in the bioactivation of aflatoxin B1, Cancer Res. 54 (1994) 101–108.
[22] Y. Fujimoto, H. Itabe, J. Sakai, M. Makita, J. Noda, M. Mori, Y. Higashi, S. Kojima, T. Takano, Identification of major proteins in the lipid droplet-enriched fraction isolated from the human hepatocyte cell line HuH7, Biochim. Biophys. Acta 1644 (2004) 47–59.
[23] S. Turro, M. Ingelmo-Torres, J.M. Estanyol, F. Tebar, M.A. Fernandez, C.V. Albor, K. Gaus, T. Grewal, C. Enrich, A. Pol, Identification and characterization of associated with lipid droplet protein 1: a novel membrane-associated protein that resides on hepatic lipid droplets, Traffic 7 (2006) 1254–1269.
[24] D.J. Murphy, The dynamic roles of intracellular lipid droplets: from archaea to mammals, Protoplasma 249 (2012) 541–585.
[25] W.S. Blaner, S.M. O'Byrne, N. Wongsiriroj, J. Kluwe, D.M. D'Ambrosio, H. Jiang, R.F. Schwabe, E.M. Hillman, R. Piantedosi, J. Libien, Hepatic stellate cell lipid droplets: a specialized lipid droplet for retinoid storage, Biochim. Biophys. Acta 1791 (2009) 467–473.
[26] D.A. Kramer, A.D. Quiroga, J. Lian, R.P. Fahlman, R. Lehner, Fasting and refeeding induces changes in the mouse hepatic lipid droplet proteome, J. Proteomics 181 (2018) 213–224.
[27] X. Zhang, Y. Wang, P. Liu, Omic studies reveal the pathogenic lipid droplet proteins in non-alcoholic fatty liver disease, Protein Cell 8 (2017) 4–13.
[28] S.K. Natarajan, K. Rasineni, M. Ganesan, D. Feng, B.L. McVicker, M.A. McNiven, N.A. Osna, J.L. Mott, C.A. Casey, K.K. Kharbanda, Structure, function and metabolism of hepatic and adipose tissue lipid droplets: implications in alcoholic liver disease, Curr. Mol. Pharmacol. 10 (2017) 237–248.
[29] S. Boulant, R. Montserret, R.G. Hope, M. Ratinier, P. Targett-Adams, J.P. Lavergne, F. Penin, J. McLauchlan, Structural determinants that target the hepatitis C virus core protein to lipid droplets, J. Biol. Chem. 281 (2006) 22236–22247.
[30] P. Roingeard, C. Hourioux, E. Blanchard, G. Prensier, Hepatitis C virus budding at lipid droplet-associated ER membrane visualized by 3D electron microscopy, Histochem. Cell Biol. 130 (2008) 561–566.
[31] A.T. Ishikawa, E.Y. Hirooka, E.S.P.L. Alvares, A. Bracarense, K. Flaiban, C.Y. Akagi, O. Kawamura, M.C.D. Costa, E.N. Itano, Impact of a single oral acute dose of aflatoxin B(1) on liver Function/Cytokines and the lymphoproliferative response in C57Bl/6 mice, Toxins (Basel). 9 (2017).
[32] J.E. Mulder, G.S. Bondy, R. Mehta, T.E. Massey, The impact of chronic Aflatoxin B1 exposure and p53 genotype on base excision repair in mouse lung and liver, Mutat. Res. 773 (2015) 63–68.
[33] N. Benkerroum, Chronic and acute toxicities of aflatoxins: mechanisms of action, Int. J. Environ. Res. Public Health 17 (2020).
[34] S. Zhang, Y. Wang, L. Cui, Y. Deng, S. Xu, J. Yu, S. Cichello, G. Serrero, Y. Ying, P. Liu, Morphologically and functionally distinct lipid droplet subpopulations, Sci. Rep. 6 (2016) 29539.
[35] M.M. Bradford, A rapid and sensitive method for the quantitation of microgram quantities of protein utilizing the principle of protein-dye binding, Anal. Biochem. 72 (1976) 248–254.
[36] A. Hanano, M. Shaban, I. Almousally, D.J. Murphy, Identification of a dioxin-responsive oxylipin signature in roots of date palm: involvement of a 9-hydroperoxide fatty acid reductase, caleosin/peroxygenase PdPXG2, Sci. Rep. 8 (2018) 13181.
[37] A. Hanano, I. Almousally, M. Shaban, F. Rahman, M. Hassan, D.J. Murphy, Specific caleosin/peroxygenase and lipoxygenase activities are tissue-differentially expressed in date palm (Phoenix dactylifera L.) seedlings and are further induced following exposure to the toxin 2,3,7,8-tetrachlorodibenzo-p-dioxin, Front. Plant Sci. 7 (2016) 2025.
[38] A. Hanano, I. Almousally, M. Shaban, Phytotoxicity effects and biological responses of Arabidopsis thaliana to 2,3,7,8-tetrachlorinated dibenzo-p-dioxin exposure, Chemosphere 104 (2014) 76–84.
[39] J. Wu, W. Xu, C. Zhang, Q. Chang, X. Tang, K. Li, Y. Deng, Trp266 determines the binding specificity of a porcine aflatoxin B(1) aldehyde reductase for aflatoxin B(1)-dialdehyde, Biochem. Pharmacol. 86 (2013) 1357–1365.
[40] W.W. Johnson, T.M. Harris, F.P. Guengerich, Kinetics and mechanism of hydrolysis of aflatoxin B1exo-8,9-Epoxide and rearrangement of the dihydrodiol, J. Am. Chem. Soc. 118 (1996) 8213–8220.
[41] T. Qiu, X. Shen, Z. Tian, R. Huang, X. Li, J. Wang, R. Wang, Y. Sun, Y. Jiang, H. Lei, et al., IgY reduces AFB1-Induced cytotoxicity, cellular dysfunction, and genotoxicity in human L-02 hepatocytes and swan 71 trophoblasts, J. Agric. Food Chem. 66 (2018) 1543–1550.
[42] X. Yang, Y. Lv, K. Huang, Y. Luo, W. Xu, Zinc inhibits aflatoxin B1-induced cytotoxicity and genotoxicity in human hepatocytes (HepG2 cells), Food Chem. Toxicol. 92 (2016) 17–25.
[43] Y.Y. Maxuitenko, T.J. Curphey, T.W. Kensler, B.D. Roebuck, Protection against aflatoxin B1-induced hepatic toxicity as short-term screen of cancer chemopreventive dithiolethiones, Fundam. Appl. Toxicol. 32 (1996) 250–259.
[44] D.H. Bechtel, Molecular dosimetry of hepatic aflatoxin B1-DNA adducts: linear correlation with hepatic cancer risk, Regul. Toxicol. Pharmacol. 10 (1989) 74–81.
[45] T. Heise, M. Schug, D. Storm, H. Ellinger-Ziegelbauer, H.J. Ahr, B. Hellwig, J. Rahnenfuhrer, A. Ghallab, G. Guenther, J. Sisnaiske, et al., In vitro - in vivo correlation of gene expression alterations induced by liver carcinogens, Curr. Med. Chem. 19 (2012) 1721–1730.
[46] F. Arenas-Huertero, M. Zaragoza-Ojeda, J. Sanchez-Alarcon, M. Milic, M. Segvic Klaric, J.M. Montiel-Gonzalez, R. Valencia-Quintana, Involvement of ahr pathway in toxicity of aflatoxins and other mycotoxins, Front. Microbiol. 10 (2019) 2347.
[47] H. Wang, D. Gilham, R. Lehner, Proteomic and lipid characterization of apolipoprotein B-free luminal lipid droplets from mouse liver microsomes: implications for very low density lipoprotein assembly, J. Biol. Chem. 282 (2007) 33218–33226.
[48] D.L. Brasaemle, G. Dolios, L. Shapiro, R. Wang, Proteomic analysis of proteins associated with lipid droplets of basal and lipolytically stimulated 3T3-L1 adipocytes, J. Biol. Chem. 279 (2004) 46835–46842.
[49] T. Tatsumi, K. Takayama, S. Ishii, A. Yamamoto, T. Hara, N. Minami, N. Miyasaka, T. Kubota, A. Matsuura, E. Itakura, et al., Forced lipophagy reveals that lipid droplets are required for early embryonic development in mouse, Development 145 (2018).
[50] A.M. Hall, E.M. Brunt, Z. Chen, N. Viswakarma, J.K. Reddy, N.E. Wolins, B.N. Finck, Dynamic and differential regulation of proteins that coat lipid droplets in fatty liver dystrophic mice, J. Lipid Res. 51 (2010) 554–563.
[51] H. Itabe, T. Yamaguchi, S. Nimura, N. Sasabe, Perilipins: a diversity of intracellular lipid droplet proteins, Lipids Health Dis. 16 (2017) 83.
[52] A. Paul, L. Chan, P.E. Bickel, The PAT family of lipid droplet proteins in heart and vascular cells, Curr. Hypertens. Rep. 10 (2008) 461–466.
[53] R.M. Carr, G. Peralta, X. Yin, R.S. Ahima, Absence of perilipin 2 prevents hepatic steatosis, glucose intolerance and ceramide accumulation in alcohol-fed mice, PLoS One 9 (2014).
[54] J.L. McManaman, E.S. Bales, D.J. Orlicky, M. Jackman, P.S. MacLean, S. Cain, A.E. Crunk, A. Mansur, C.E. Graham, T.A. Bowman, Perilipin-2-null mice are protected against diet-induced obesity, adipose inflammation, and fatty liver disease, J. Lipid Res. 54 (2013) 1346–1359.
[55] K.T. Dalen, S.M. Ulven, B.M. Arntsen, K. Solaas, H.I. Nebb, PPARα activators and fasting induce the expression of adipose differentiation-related protein in liver, J. Lipid Res. 47 (2006) 931–943.
[56] R. Mishra, S.N. Emancipator, C. Miller, T. Kern, M.S. Simonson, Adipose differentiation-related protein and regulators of lipid homeostasis identified by gene expression profiling in the murine db/db diabetic kidney, Am. J. Physiol. Renal Physiol. 286 (2004) F913–F921.
[57] W. Motomura, M. Inoue, T. Ohtake, N. Takahashi, M. Nagamine, S. Tanno, Y. Kohgo, T. Okumura, Up-regulation of ADRP in fatty liver in human and liver steatosis in mice fed with high fat diet, Biochem. Biophys. Res. Commun. 340 (2006) 1111–1118.
[58] J. Gong, Z. Sun, L. Wu, W. Xu, N. Schieber, D. Xu, G. Shui, H. Yang, R.G. Parton, P. Li, Fsp27 promotes lipid droplet growth by lipid exchange and transfer at lipid droplet contact sites, J. Cell Biol. 195 (2011) 953–963.
[59] K. Lapid, J.M. Graff, Form(ul)ation of adipocytes by lipids, Adipocyte 6 (2017) 176–186.
[60] L.N.Z. Ramalho, L.D. Porta, R.E. Rosim, T. Petta, M.J. Augusto, D.M. Silva, F.S. Ramalho, C.A.F. Oliveira, Aflatoxin B1 residues in human livers and their relationship with markers of hepatic carcinogenesis in Sao Paulo, Brazil, Toxicol. Rep. 5 (2018) 777–784.
[61] H. Green, M. Meuth, An established pre-adipose cell line and its differentiation in culture, Cell 3 (1974) 127–133.
[62] O. Pepicelli, E. Fedele, M. Berardi, M. Raiteri, G. Levi, A. Greco, M.A. Ajmone-Cat, L. Minghetti, Cyclo-oxygenase-1 and -2 differently contribute to prostaglandin E2 synthesis and lipid peroxidation after in vivo activation of N-methyl-D-aspartate receptors in rat hippocampus, J. Neurochem. 93 (2005) 1561–1567.
[63] J.E. Goodman, E.D. Bowman, S.J. Chanock, A.J. Alberg, C.C. Harris, Arachidonate lipoxygenase (ALOX) and cyclooxygenase (COX) polymorphisms and colon cancer risk, Carcinogenesis 25 (2004) 2467–2472.
[64] J. Wu, R. Chen, C. Zhang, K. Li, W. Xu, L. Wang, Q. Chen, P. Mu, J. Jiang, J. Wen, et al., Bioactivation and regioselectivity of pig cytochrome P450 3A29 towards aflatoxin B(1), Toxins (Basel). 8 (2016).
[65] S.A. Khan, E.E. Wollaston-Hayden, T.W. Markowski, L. Higgins, D.G. Mashek, Quantitative analysis of the murine lipid droplet-associated proteome during diet-induced hepatic steatosis, J. Lipid Res. 56 (2015) 2260–2272.

[66] A.E. Crunk, J. Monks, A. Murakami, M. Jackman, P.S. Maclean, M. Ladinsky, E.S. Bales, S. Cain, D.J. Orlicky, J.L. McManaman, Dynamic regulation of hepatic lipid droplet properties by diet, PLoS One 8 (2013) e67631.
[67] M. Liu, R. Ge, W. Liu, Q. Liu, X. Xia, M. Lai, L. Liang, C. Li, L. Song, B. Zhen, et al., Differential proteomics profiling identifies LDPs and biological functions in high-fat diet-induced fatty livers, J. Lipid Res. 58 (2017) 681–694.
[68] P.J. Klein, R. Buckner, J. Kelly, R.A. Coulombe Jr., Biochemical basis for the extreme sensitivity of turkeys to aflatoxin B(1), Toxicol. Appl. Pharmacol. 165 (2000) 45–52.
[69] P.J. Klein, T.R. Van Vleet, J.O. Hall, R.A. Coulombe Jr., Biochemical factors underlying the age-related sensitivity of turkeys to aflatoxin B(1), Comp. Biochem. Physiol. C Toxicol. Pharmacol. 132 (2002) 193–201.
[70] P.J. Klein, T.R. Van Vleet, J.O. Hall, R.A. Coulombe Jr., Dietary butylated hydroxytoluene protects against aflatoxicosis in Turkeys, Toxicol. Appl. Pharmacol. 182 (2002) 11–19.
[71] D.L. Eaton, E.P. Gallagher, Mechanisms of aflatoxin carcinogenesis, Annu. Rev. Pharmacol. Toxicol. 34 (1994) 135–172.
[72] J.A. Guarisco, J.O. Hall, R.A. Coulombe Jr., Butylated hydroxytoluene chemoprevention of aflatoxicosis - effects on aflatoxin B(1) bioavailability, hepatic DNA adduct formation, and biliary excretion, Food Chem. Toxicol. 46 (2008) 3727–3731.
[73] Z. Ilic, T.K. Mondal, I. Guest, D.R. Crawford, S. Sell, Participation of liver stem cells in cholangiocarcinogenesis after aflatoxin B1 exposure of glutathione S-transferase A3 knockout mice, Tumour Biol. 40 (2018) 1010428318777344.
[74] A.P. Magnoli, M.L. Gonzalez Pereyra, M.P. Monge, L.R. Cavaglieri, S.M. Chiacchiera, Validation of a liquid chromatography/tandem mass spectrometry method for the detection of aflatoxin B1 residues in broiler liver, Rev. Argent. Microbiol. 50 (2018) 157–164.